Available online at www.sciencedirect.com
ScienceDirect
Physica E 35 (2006) 257–263
PHYSICA E
www.elsevier.com/locate/physe

Electron spin coherence in Si

A.M. Tyryshkin[a], S.A. Lyon[a,*], T. Schenkel[b], J. Bokor[c], J. Chu[d], W. Jantsch[e], F. Schäffler[e], J.L. Truitt[f], S.N. Coppersmith[f], M.A. Eriksson[f]

[a]*Department of Electrical Engineering, Princeton University, Princeton, NJ 08544, USA*
[b]*E O Lawrence Berkeley National Laboratory, Berkeley, CA 94720, USA*
[c]*Department of Electrical Engineering and Computer Science, University of California, Berkeley, CA 94720, USA*
[d]*IBM Research Division, T.J. Watson Research Center, Yorktown Heights, NY 10598, USA*
[e]*Institute für Halbleiter-und Festkörperphysik, Johannes-Kepler-Universität Linz, A-4040, Austria*
[f]*Physics Department, University of Wisconsin-Madison, USA*

Available online 30 October 2006

Abstract

We discuss pulsed electron spin resonance measurements of electrons in Si and determine the spin coherence from the decay of the spin echo signals. Tightly bound donor electrons in isotopically enriched ^{28}Si are found to have exceptionally long spin coherence. Placing the donors near a surface or interface is found to decrease the spin coherence time, but it is still in the range of milliseconds. Unbound two-dimensional electrons have shorter coherence times of a few microseconds, though still long compared to the Zeeman frequency or the typical time to manipulate a spin with microwave pulses. Longer spin coherence is expected in two-dimensional systems patterned into quantum dots, but relatively small dots will be required. Data from dots with a lithographic size of 400 nm do not yet show longer spin coherence.

PACS: 03.67.Lx; 76.30.−v; 73.21.Fg

Keywords: Spin resonance; Spin relaxation; Spin coherence; Quantum computing

1. Introduction

One of the key requirements for a two-level quantum system to be considered as a good qubit for quantum computation is that it have low decoherence [1]. Spin systems are natural candidates, since their magnetic dipoles tend to interact with the environment much more weakly than states which involve charge motion. Nuclear spins are known to have long coherence times, but their magnetic moments are inconveniently small. The electron magnetic moment is three orders of magnitude larger than the nuclear moment, but that also makes electron spins more susceptible to decoherence. However, a combination of factors makes electron spins in silicon crystals uncommonly good qubits. The spin–orbit interaction in silicon is particularly small, partly because it is a light element and partly due to the Si band structure [2]. In addition, natural Si has a low ($<5\%$) abundance of isotopes with nonzero magnetic moment, which can be reduced further. Si crystals can be manufactured with exceptional purity and a low density of defects. Finally, there is a huge technological base built up around the control and movement of electrons in Si.

Well before silicon became the dominant material for the semiconductor industry, even before there was a semiconductor industry to speak of, Si was an important proving ground for electron spin resonance (ESR) experiments [3–6]. Electron nuclear double resonance was invented originally for the purpose of understanding the ESR of donor impurities in Si [7], and the first microwave spin-echo was measured from electrons bound to silicon donors [8]. In more heavily doped Si the interactions between donors led to the Anderson theory of localization

*Corresponding author. Fax: +1 609 258 6279.
E-mail address: lyon@princeton.edu (S.A. Lyon).

1386-9477/$ - see front matter © 2006 Elsevier B.V. All rights reserved.
doi:10.1016/j.physe.2006.08.021

[9]. However, as ESR understanding and techniques evolved, interest shifted to more complex systems; defects in materials as well as organic and biological molecules.

Quantum computation will require highly complex systems, but made up from large numbers of well-characterized two-level systems. Precisely controlled spin manipulation and spin–spin interactions are necessary leading one to consider relatively slow processes, and thus long coherence times are needed. These unique requirements for quantum information processing have led to a resurgence of interest in understanding the "simple" systems, such as electron spins in silicon.

In this paper we will discuss results of pulsed-ESR measurements of spin relaxation in various Si structures. We have found that the spin coherence of electrons bound to isolated shallow donors in isotopically enriched silicon (extrapolating to the single donor situation) can be as long as 60 ms at 6.9 K [10]. Ion implanting donors into Si leaving the impurities near a surface or interface, produces shorter coherence times, which are found to depend upon how the surface is treated. Etching in hydrofluoric acid, leaving a hydrogen-terminated surface, results in longer coherence than an oxidized surface [11]. In high mobility two-dimensional electron systems (2DES) we find shorter relaxation times, of the order of a few microseconds because the electrons are now unconfined in two directions and are susceptible to decoherence through the spin–orbit interaction [12]. Unlike the donors, which have a ground state that is only spin degenerate, the 2DES allows excitations with vanishingly small energy. This argument suggests that lithographic patterning of the 2DES into quantum dots can be expected to restore the spin coherence to that of the donor, which can be viewed as a "natural" quantum dot. Measurements of dots with lateral dimensions down to 400 nm do not show an increase in spin coherence, and elementary considerations lead us to conclude that these dots are not yet at the quantum limit, and smaller dots are needed.

2. Donor electron spins

The spin of an electron bound to a donor is a natural candidate as a qubit [13]. The ground state of most of the shallow donors in Si (all except for Li) is nondegenerate, except for spin. There is also a large energy splitting to the lowest excited states (about 10 meV or more for the common donors), which helps protect the spin from decoherence associated with spin–orbit coupling [14,15]. A half century ago it was already known that the longitudinal relaxation time (spin flip time), T_1, could be many minutes at low temperatures (~1 K) [4]. The spin coherence was measured to be considerably shorter; about 200 μs in natural Si, rising to ~520 μs in isotopically enriched ^{28}Si [8].

In natural Si the spin echo decay is nonexponential [8,10,16]. The origins of the decoherence are the fluctuations of the nuclear magnetic moments of the ^{29}Si [16–18]. The electrons are coupled to the nuclei, either through the hyperfine interaction or through the magnetic dipole-dipole interaction. The fluctuating nuclear moments lead to spectral diffusion of the electron spin, which appears as a nonexponential loss of echo amplitude.

Isotopically enriched ^{28}Si is readily available with ^{29}Si (the only stable isotope with a nuclear magnetic moment) concentrations in the range of 800 ppm. Care must be taken to avoid small fluctuating magnetic fields in the environment, but with suitable attention to these details the spin echo decays are exponential [10]. In Fig. 1 we show an Arrhenius plot of the measured spin echo decay time, T_2, for ^{28}Si:P with two different doping densities, 10^{15} and $10^{16}\,\mathrm{cm}^{-3}$. Also plotted in the figure is the temperature dependence of T_1. T_1 is found to be independent of doping concentration, and through this temperature range the longitudinal relaxation rate falls exponentially with inverse temperature. This indicates that the relaxation is controlled by an Orbach process, as had been seen earlier [15,19]. The gap is 126 K, which corresponds to the splitting to the lowest excited states (valley-orbit split states) of the donor. At higher temperatures the T_2 measured for both samples are the same as T_1, and we can conclude that this same Orbach process is also controlling the decoherence. However, at lower temperatures the decoherence rate stops dropping exponentially and saturates at a fixed value. An important observation is that the saturation T_2 in the sample with $10^{15}\,\mathrm{cm}^{-3}$ phosphorus is an order of magnitude lower than that in the $10^{16}\,\mathrm{cm}^{-3}$ doped sample. This gives us a clue that the low-temperature decoherence is being limited by interactions between the electron spins.

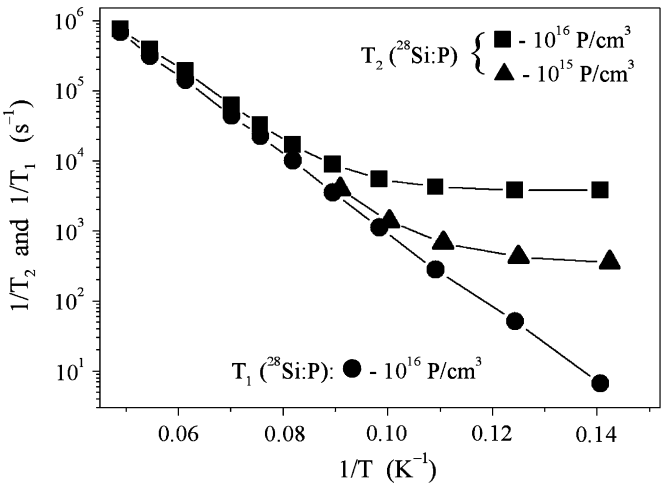

Fig. 1. An Arrhenius plot of measured spin relaxation rates, $1/T_1$ (solid circles) and $1/T_2$ for two different phosphorus doping levels in enriched ^{28}Si; $10^{16}\,\mathrm{cm}^{-3}$ (solid squares) and $10^{15}\,\mathrm{cm}^{-3}$ (solid triangles). The data for $1/T_1$ are the same for both samples, and only one set is shown. The lines are just guides to the eye. The longitudinal relaxation rate, $1/T_1$, is controlled by the Orbach process over the entire temperature range, and those points fall on a straight line. At higher temperatures, all three curves fall on the same straight line, but the T_2 data saturate at lower temperatures, with the $1/T_2$ saturating at about an order of magnitude faster rate in the more heavily doped sample (after Ref. [10]).

One aspect of the dipole–dipole interaction is termed "instantaneous diffusion" and arises from the fact that in the typical two-pulse Hahn echo pulse sequence the second (refocusing) pulse rotates all of the spins by 180° [20,21]. If one spin feels the magnetic field of another (magnetic dipole–dipole interaction), when the spins are all flipped the sign of the local dipole field also changes. Thus the echo sequence does not refocus this interaction in the same way as simple static inhomogeneities. However, by decreasing the magnitude of the second microwave pulse, the probability of flipping both spins is reduced In this case the echo is produced only by those spins which are flipped, while the other nearby spins are not flipped and their interaction is reduced to a static one. Of course, refocusing fewer spins reduces the signal, but in the limit of a vanishing second pulse the echo decay will be that of isolated spins. A plot demonstrating this technique for donor electrons in Si is shown in Fig. 2. This data was obtained at 6.9 K with a 25 μm thick epitaxial layer of ^{28}Si:P uniformly-doped to $9\times10^{14}\,\mathrm{cm}^{-3}$. The echo decay rate is seen to decrease as the turning angle (θ) of the second (refocusing) microwave pulse is decreased. We plot the decay rate vs. $\sin^2(\theta/2)$ since this quantity is proportional to the probability that a spin is flipped by the refocusing pulse. The data fit a straight line well, as expected, and the intercept at zero turning angle is 60 ms. This time can be interpreted as the intrinsic decoherence time for an isolated phosphorus donor bound electron in Si. The open circle symbol shown just below the intercept corresponds to the measured T_1 (280 ms) in this sample

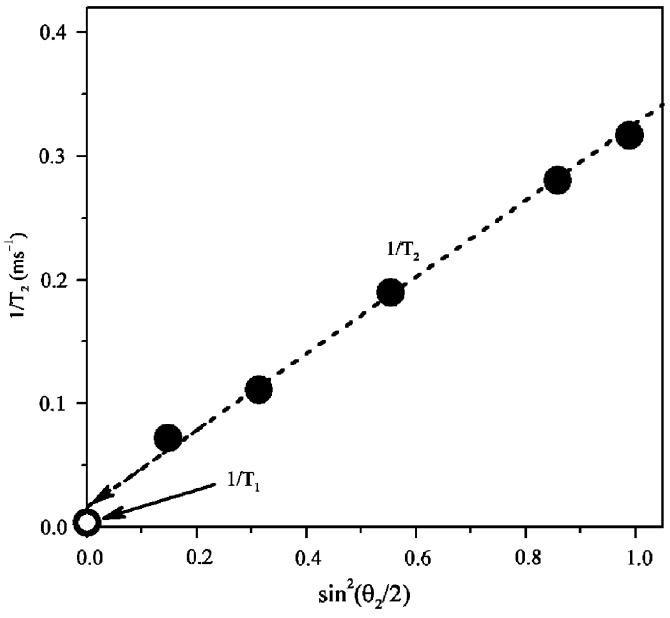

Fig. 2. A plot of the transverse relaxation rate, $1/T_2$, versus $\sin^2(\theta_2/2)$ in a ^{28}Si:P sample doped at $9\times10^{14}\,\mathrm{cm}^{-3}$, where θ_2 is the angle through which the spins are rotated by the second pulse of a two-pulse Hahn echo sequence. The intercept at $\theta_2=0$ is 60 ms, the extrapolated relaxation rate of a single isolated spin. The circle shown on the plot, and labeled "$1/T_1$" is the longitudinal relaxation rate measured on this sample under the same conditions as the T_2 data. The value of T_1 is 280 ms (after Ref. [10]).

under the same conditions. T_1 is not affected by the either the residual ^{29}Si nuclear moments or the dipole-dipole interactions between the electron spins. It is not certain, but it may be that the 800 ppm of ^{29}Si still in this enriched ^{28}Si is limiting the coherence time. If so, with further reductions in the ^{29}Si density and lower temperatures, even longer spin coherence times may be possible.

The results on the pristine epitaxial layers of ^{28}Si show long spin coherence, but real devices will require significant processing. To address individual spins with gates while keeping the spins close enough together to allow controlled interactions between them necessitates the donors being placed close to the gates; thus close to a surface or interface. To test how interfaces and limited processing affects the spin coherence we have measured T_1 and T_2 of donor bound electrons which have been implanted at low energy into undoped ^{28}Si epitaxial layers [11]. The impurity chosen is ^{121}Sb, since it is easier to control the depth of the implanted impurities for a heavier element and there is no confusion from unintentional background phosphorus doping. Standard CMOS processes were used to form 5 to 10 nm thermal oxides on the Si, and the Sb ions were then implanted with energies of 120 and 400 keV at a dose of $2\times10^{11}\,\mathrm{cm}^{-2}$. After implantation the samples were rapid-thermal-annealed for 7–10 s at 980–1000 °C in N_2 or N_2/H_2 ambients. Secondary ion mass spectrometry and spreading resistance analysis were used to determine the final Sb depth profiles. Both showed that after the anneal the Sb distribution of the deeper (400 keV) implant was centered about 150 nm below the surface, with nearly 100% electrical activation but the annealing introduced significant broadening. The shallower (120 keV) implanted and annealed distribution was centered closer to the surface (about 50 nm) as determined by SIMS, and it accurately matched the calculated implant profile. Electrical measurements showed that the activation was only ~3%. These shallow implants also showed a negligible ESR signal upon cooling, but after illuminating them at low temperature the ESR signal increased significantly. This effect, and the apparent low activation might both result from carrier trapping at the nearby Si/SiO_2 interface which had an interface state density of $1-2\times10^{11}\,\mathrm{cm}^{-2}$.

In Fig. 3 we show a typical pulsed-ESR measurement of spin echo decay of the electrons bound to ^{121}Sb donors in the deeper (400 keV) implanted sample. The inset shows the cw ESR absorption signal, with the six sharp hyperfine lines coming from six different projections of the ^{121}Sb nuclear spin $I=\frac{5}{2}$. The broad line in the center of the spectrum arises from unpaired electrons bound to defects introduced through the processing, but these spins decohere rapidly and do not interfere with the pulsed measurements. The spin number in these sample is not large enough to use the techniques we had developed to counter the effects of environmental magnetic field noise, and thus the echo decay becomes nonexponential after about 0.5–1 ms. However, we have fit the first, exponential portion, of the decay to extract a T_2 of 2.1 ms in this

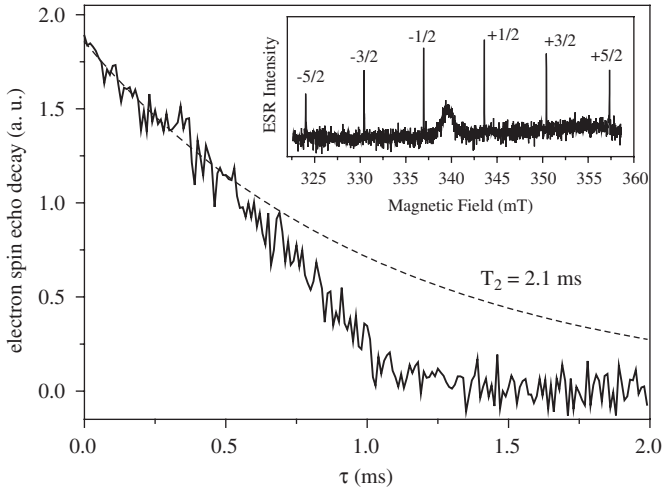

Fig. 3. A spin echo decay (echo amplitude versus time) measured on Sb-implanted ^{28}Si. This sample was implanted at 400 keV, annealed at 980 °C for 7 s. The oxide was etched off in hydrofluoric acid before recording this trace. The nonexponential decay observed after about 0.5 ms arises from environmental noise, but there was insufficient signal to eliminate this effect. The dashed curve is an exponential fit to the short-time portion of the data. The inset is a cw-ESR spectrum of this sample, showing the six hyperfine lines of the Sb.

Table 1
Summary of activation ratios and spin relaxation times for 120 and 400 keV implantation energies, as well as the results with the oxide capping layer (SiO_2) on the samples and etched off in hydrofluoric acid (H–Si)

Interface	Peak dopant depth (nm)	Apparent activation ratio (%)	T_1 (ms) at 5.2 K	T_2 (ms) at 5.2 K
SiO_2	50	3.4	15 ± 2	0.30 ± 0.03
H–Si	50	—	16 ± 2	0.75 ± 0.04
SiO_2	150	100	16 ± 1	1.5 ± 0.1
H–Si	150	—	14 ± 1	2.1 ± 0.1

structure. In this plot we have not reduced the amplitude of the second microwave pulse, as was done for Fig. 2, and thus instantaneous diffusion has not been eliminated. We did find that reducing the turning angle of the second pulse produced longer echo decays, so that instantaneous diffusion is contributing to the measured decoherence, but the decay does not reach 60 ms. Thus other, as yet unknown, relaxation processes are also contributing to the decoherence.

The decay shown in Fig. 3 was obtained after etching the SiO_2 layer off in hydrofluoric acid, leaving a hydrogen-terminated surface (though hydrogen termination is less effective on this (1 0 0) surface than on (1 1 1) surfaces). Before etching off the oxide, this sample gave a coherence time of 1.5 ms. Thus we can conclude that the nearby oxide layer introduces decoherence, probably though fast-relaxing paramagnetic defects. In Table 1 we give the T_1 and T_2 results for both samples (120 and 400 keV implants) and both before and after oxide removal. T_1 is found to be about the same, ~15 ms in all cases, but T_2 is not. The coherence time is shorter for the shallower implant, but increases after oxide removal for both samples. To conclude, while the coherence time has been shortened by the implantation and associated processing, it is still quite long, and there is evidence that it can be made longer.

3. Two-dimensional electrons' spins

In some proposals for electron-spin based quantum computing the electrons are confined in quantum wells or heterostructures, which are then structured into quantum dots [22–25]. Others involve pulling electrons from donor atoms towards a heterointerface, to change their interactions, or to move them from donor to donor [13,26,27]. However, there have been few measurements of spin coherence in such structures, particularly for Si. The first step in that direction is to measure the spin coherence of two-dimensional electrons. One might expect that in an unpatterned 2DES the spin–orbit interaction will be more important than for the donors, since there is no gap to the excited states. That is what we observe [12], as shown in Fig. 4. The samples consist of high mobility electrons (90,000 $cm^2/V\,s$ at low temperature) MBE-grown in a modulation-doped Si quantum wells in SiGe. The quantum wells were 20 nm wide, and they were grown on strain-relaxed SiGe with 25% Ge. The structures were illuminated at low temperature, producing an electron density of about $3\times10^{11}\,cm^{-2}$. The upper part of the figure shows the results of an inversion recovery experiment to measure T_1, and the lower panel shows the echo decay measurement of T_2, with the magnetic field, B_0, oriented perpendicular to the plane of the 2DES in both experiments. If the magnetic field is oriented in the plane of the 2DES, T_1 increases to 3 μs, while T_2 decreases to about 0.3 μs. These results are consistent with a model of the spin relaxation in which the electrons experience a fluctuating effective magnetic field arising from the Rashba effect [28] which was devised to explain extensive cw-ESR data [29–36]. This effective field is oriented perpendicular to the wave vector of the electron, and always lies in the plane of the 2DES. With the external magnetic field perpendicular to this plane, the Rashba field causes purely longitudinal relaxation, which accounts for the fact that $T_2 > T_1$ (since we do not find $T_2 = 2T_1$, there must be another relaxation mechanism at work, as well). The mobility of this structure corresponds to a momentum relaxation time of about 10 ps, which together with the measured T_1 and T_2 implies a Rashba field of about 10 Gauss. With the magnetic field in the plane of the electrons, the part of the Rasba field which is perpendicular to B_0 causes longitudinal relaxation, while that part of the fluctuating field which is parallel to B_0 only affects T_2.

As long as the electrons are free to scatter, one expects that the spin–orbit interaction will limit the spin coherence times. However, if lithographic quantum dots are fabricated in a 2DES, the effect of the Rashba field will be reduced. In the limit of a single electron in the

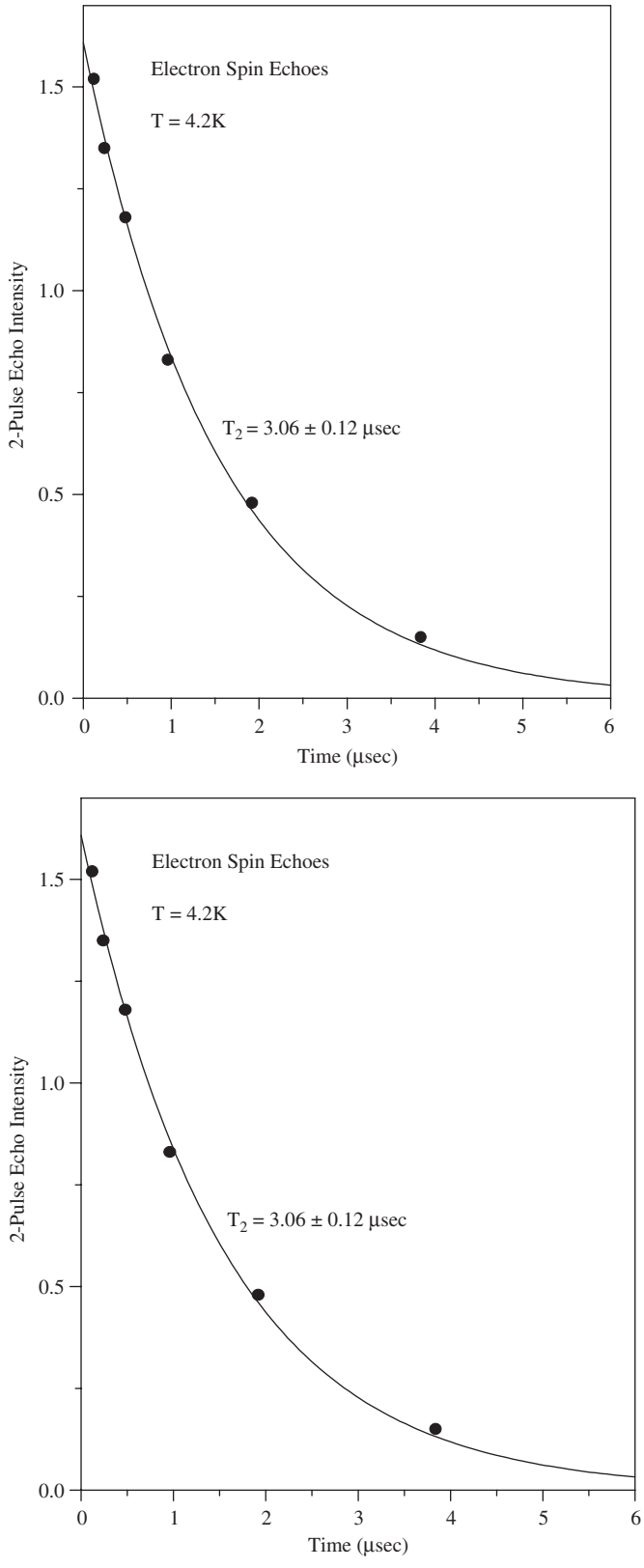

Fig. 4. Spin relaxation of 2D electrons for the sample with an electron density of $3 \times 10^{11}\,\mathrm{cm}^{-2}$ and mobility of $90{,}000\,\mathrm{cm}^2/\mathrm{V\,s}$. The data were measured at 4.2 K with the magnetic field normal to the plane of the 2DES. The upper panel shows the results of an inversion-recovery experiment to measure T_1. The line is an exponential fit to the data points, and gives $T_1 = 1.95\,\mu\mathrm{s}$. The lower panel shows the data from a two-pulse spin echo experiment. The line is an exponential fit to the data points, and gives $T_2 = 3.06\,\mu\mathrm{s}$.

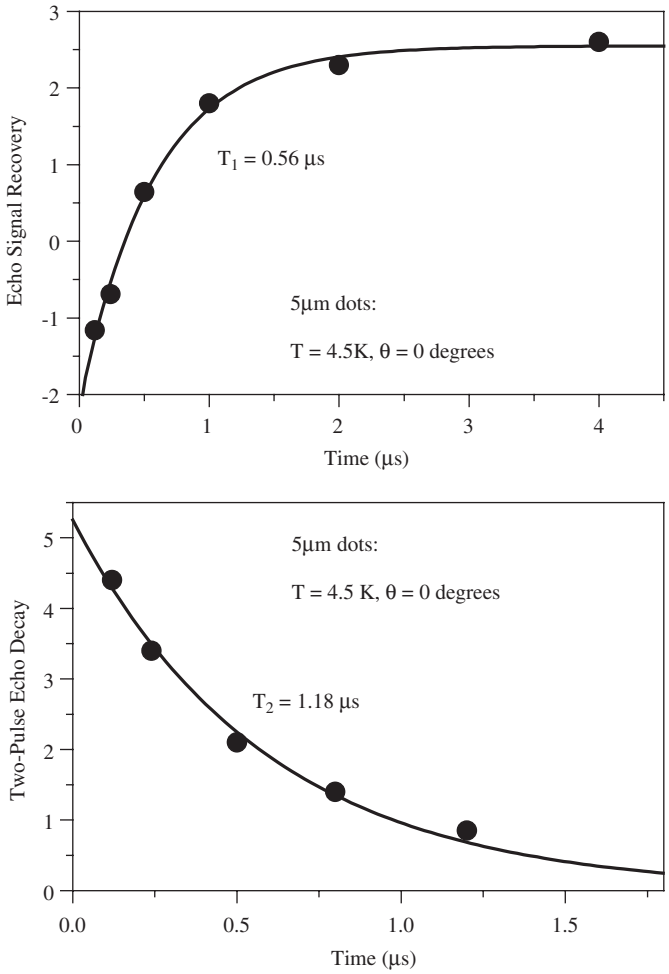

Fig. 5. Spin relaxation measured for 5 μm dots etched into a 2D electron system with a pre-etch electron density of $4 \times 10^{11}\,\mathrm{cm}^{-2}$ and a mobility of $37{,}300\,\mathrm{cm}^2/\mathrm{V\,s}$. The data were measured at 4.5 K with the magnetic field normal to the plane of the 2DES. The upper panel shows the results of an inversion-recovery experiment to measure T_1. The line is an exponential fit to the data points, and gives $T_1 = 0.56\,\mu\mathrm{s}$. The lower panel shows the data from a two-pulse spin echo experiment. The line is an exponential fit to the data points, and gives $T_2 = 1.18\,\mu\mathrm{s}$. There are evidently small experimental errors in these numbers, since it is not possible to have $T_2 > 2T_1$.

nondegenerate ground state of a quantum dot, the spin coherence could approach that of the donor-bound electrons (the donors can be thought of as "natural quantum dots"). In Fig. 5 we show pulsed-ESR measurements of T_1 (upper panel) and T_2 (lower panel) for large, 5 μm dots. The dots were formed by etching a 2DES with an electron density of $4 \times 10^{11}\,\mathrm{cm}^{-2}$ and a low-field mobility of $37{,}300\,\mathrm{cm}^2/\mathrm{V\,s}$ [37]. These structures were grown by CVD, with a quantum well of width 8 nm on a relaxed SiGe with 25% Ge. Here we find that $T_1 \sim 0.6\,\mu\mathrm{s}$ while $T_2 \sim 1.2\,\mu\mathrm{s}$. These relaxation times are essentially the same as those measured on the unpatterned 2DES from which these dots were made. In these samples we see that $T_2 \sim 2T_1$ which implies that the relaxation process is purely longitudinal and the Rashba effect alone can account for the spin relaxation. The effective magnetic field from the

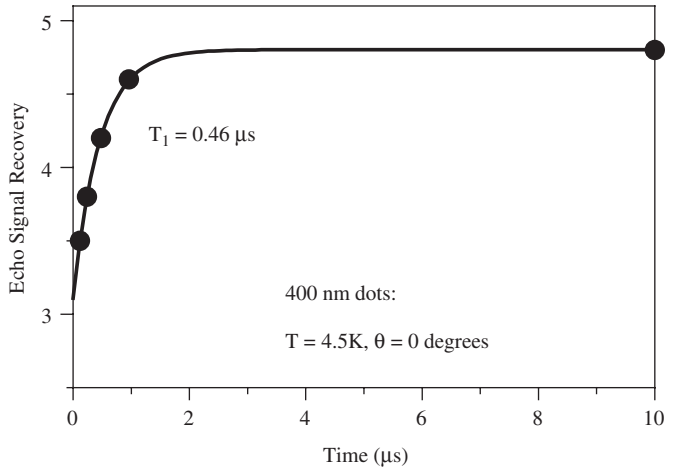

Fig. 6. Longitudinal spin relaxation measured for 400 nm dots etched into a 2D electron system with a pre-etch electron density of $4 \times 10^{11}\,\mathrm{cm}^{-2}$ and a mobility of $37{,}200\,\mathrm{cm}^2/\mathrm{V\,s}$. The data were measured at 4.5 K with the magnetic field normal to the plane of the 2DES. The plot shows the results of an inversion-recovery experiment to measure T_1. The line is an exponential fit to the data points, and gives $T_1 = 0.46\,\mu\mathrm{s}$.

Rashba effect needed to account for these relaxation rates is about 26 Gauss.

In Fig. 6 we show the inversion recovery results (T_1) for smaller dots etched into the same starting 2DES material. The lithographic size of these dots is 400 nm, though edge depletion may make the region in which the electrons are confined slightly smaller. One might expect that these dots are approaching the quantum limit. However, we obtain a T_1 of 0.46 μs, which is comparable to but slightly shorter than that measured on the large dots. The spin echo signals were too weak to measure T_2, but we know that it can be no longer than twice T_1. It appears that the spin relaxation in these dots is the same as it is in the unpatterned 2DES. The fact that we are not seeing longer T_1 and T_2 times in the existing dots can be understood by considering the mean free path of an electron in this material. From the mobility and electron density we find that an electron at the Fermi surface relaxes its momentum in about 300 nm. This is similar to or smaller than the size of the dot, and these structures are not yet truly quantum. Thus it is not unexpected that the spin relaxation will be similar to that observed in the bulk 2DES. Smaller dots will be needed to obtain longer coherence times.

From an architectural perspective it would be advantageous in a quantum computer to have the ability to move the qubits (individual electron spins for our purposes), though that is not required [38–40]. With a spin coherence time of a few microseconds in a 2DES a spin could be moved long distances before it decoheres; of the order of 10 cm for a 1 μs coherence time and velocity of 10^7 cm/s. However, to maintain fault tolerance a future quantum processor can only allow a small probability (likely about 0.01%) of a spin losing coherence [41], and thus one is limited to motion of ~10 μm. This distance is already large compared to projected qubit dimensions [13]. However, if longer coherence times can be obtained for unbound electrons, then global communications within a quantum computer would be possible by simply moving the electron spin qubits. There are several possible approaches to increasing the coherence time of 2D electrons in Si quantum wells. One would be to reduce the asymmetry, and thus decrease the effective Rashba field. However, the two 2DES structures discussed above were grown in rather different manners, but have similar spin coherence times. It is not yet clear how the growth should be changed to increase the spin coherence. Another possibility would be to decrease the mobility of the 2D electrons. As the electrons scatter their spin sees a fluctuating effective magnetic field. If the electron scatters more rapidly, the fluctuations will be smaller and averaged more rapidly [42]. This is analogous to the motional narrowing observed for nuclear spins in liquids. For example, if the 2DES used for Fig. 4 had its mobility reduced from 90,000 to $1000\,\mathrm{cm}^2/\mathrm{V\,s}$, with everything else remaining the same, the T_2 from the Rashba effect would be over 100 μs. Such a mobility is comparable to the room temperature electron mobility in Si transistors, and thus would not seriously affect the maximum velocities at which the electrons could be moved. At some point Elliott–Yafet spin relaxation will become important, and reduce spin coherence with further reductions in mobility, but it is not certain when that will become important [43–45]. Work is underway to test whether longer spin coherence can be obtained in lower mobility structures.

4. Conclusions

We have seen that exceptionally long spin coherence can be obtained in Si-based structures. To the best of our knowledge, the spin echo decays measured for electrons bound to donors in ^{28}Si represent the longest electron spin coherence times ever observed. Even after ion implantation, annealing, and being placed near an interface, the donors still have coherence times of over a millisecond. A nearby Si/SiO_2 interface reduces the spin coherence as compared to a hydrogen-terminated surface, but it is not yet known definitively what is causing the extra decoherence from the oxide. Work is underway to understand this issue.

Without the large gap to an excited state the spin coherence of electrons in a 2DES is shorter than for the donors. However, it is still of the order of a few microseconds. The pulsed-ESR data are consistent with a picture developed to explain cw ESR results in which the spins are subject to a fluctuating effective Rashba magnetic field arising form the spin–orbit interaction and the broken symmetry at a heterointerface. The effect on the spin coherence of this Rashba field is expected to be reduced in a confined geometry, such as a quantum dot, but small dots will be required to verify this expectation. Measurements of 400 nm dots etched into a 2DES do not yet show enhanced spin coherence.

Acknowledgments

The work in Princeton was supported in part by ARO and ARDA under Contract No. DAAD19-02-1-0040 and DARPA's SPINS Program through Los Alamos National Laboratory. The work at Berkeley was supported by NSA under ARO Contract No. MOD707501 and the Department of Energy under Contract No. DE-AC02-05CH11231. The work in Linz was supported by the *Fonds zur Förderung der Wissenschaftlichen Forschung,* the ÖAD, and the GMe in Vienna. The work at Wisconsin was supported by ARO, ARDA, NSA, and NSF.

References

[1] D.P. DiVincenzo, Fortschr. Phys. 48 (2000) 771.
[2] L. Liu, Phys. Rev. Lett. 6 (1961) 683.
[3] G. Feher, Phys. Rev. 114 (1959) 1219.
[4] G. Feher, E.A. Gere, Phys. Rev. 114 (1959) 1245.
[5] A. Honig, Phys. Rev. 96 (1954) 234.
[6] A. Honig, J. Combrisson, Phys. Rev. 102 (1956) 917.
[7] G. Feher, Phys. Rev. 103 (1956) 834.
[8] J.P. Gordon, K.D. Bowers, Phys. Rev. Lett. 1 (1958) 368.
[9] P.W. Anderson, Nobel Lect. (1977).
[10] A.M. Tyryshkin, et al., Phys. Rev. B 68 (2003) 193207.
[11] T. Schenkel, et al., Appl. Phys. Lett. 88 (2006) 112101.
[12] A.M. Tyryshkin, et al., Phys. Rev. Lett. 94 (2005) 126802.
[13] B.E. Kane, Nature 393 (1998) 133.
[14] T.G. Castner, Phys. Rev. Lett. 8 (1962) 13.
[15] T.G. Castner, Phys. Rev. 155 (1967) 816.
[16] M. Chiba, A. Hirai, J. Phys. Soc. Japan 33 (1972) 730.
[17] J.R. Klauder, P.W. Anderson, Phys. Rev. 125 (1962) 912.
[18] R. de Sousa, S. Das Sarma, Phys. Rev. B 68 (2003) 115322.
[19] R. Orbach, Proc. Phys. Soc. London 77 (1961) 821.
[20] A.M. Raitsimring, et al., Sov. Phys. Solid State 16 (1974) 492.
[21] K.M. Salikhov, S.A. Dzuba, A.M. Raitsimring, J. Magn. Reson. 42 (1981) 255.
[22] M. Friesen, et al., Phys. Rev. B 67 (2003) 121301.
[23] D. Loss, D.P. DiVincenzo, Phys. Rev. A 57 (1998) 120.
[24] J.R. Petta, et al., Science 309 (2005) 2180.
[25] R. Vrijen, et al., Phys. Rev. A 62 (2000) 012306.
[26] B.E. Kane, Fortschr. Phys. 48 (2000) 1023.
[27] A.J. Skinner, M.E. Davenport, B.E. Kane, Phys. Rev. Lett. 90 (2003) 087901.
[28] Y.A. Bychkov, E.I. Rashba, J. Phys. C 17 (1984) 6039.
[29] W. Jantsch, et al., Phys. Stat. Sol. B 210 (1998) 643.
[30] W. Jantsch, et al., Physica E 6 (2000) 218.
[31] N. Sandersfeld, et al., Thin Solid Films 369 (2000) 312.
[32] Z. Wilamowski, et al., Phys. Rev. Lett. 8702 (2001).
[33] W. Jantsch, et al., Physica E 13 (2002) 504.
[34] Z. Wilamowski, W. Jantsch, Physica E 12 (2002) 439.
[35] Z. Wilamowski, et al., Phys. Rev. B 66 (2002).
[36] Z. Wilamowski, et al., Physica E 16 (2003) 111.
[37] J.L. Truitt, Spin coherence in silicon/silicon–germanium nanostructures, Ph.D. Thesis, University of Wisconsin-Madison, Madison, 2004.
[38] K.M. Svore, B.M. Terhal, D.P. DiVincenzo, Phys. Rev. A 72 (2005) 022317.
[39] A.G. Fowler, S.J. Devitt, L.C.L. Hollenberg, arXiv:quant-ph/0402196 (2004).
[40] A.G. Fowler, C.D. Hill, L.C.L. Hollenberg, arXiv:quant-ph/0311116 (2003).
[41] A.M. Steane, arXiv:quant-ph/0207119 (2004).
[42] J.M. Kikkawa, D.D. Awschalom, Phys. Rev. Lett. 80 (1998) 4313.
[43] R. Elliott, Phys. Rev. 96 (1954) 266.
[44] Y. Yafet, Solid State Phys. 14 (1963) 1.
[45] Z. Wilamowski, W. Jantsch, Phys. Rev. B 69 (2004).